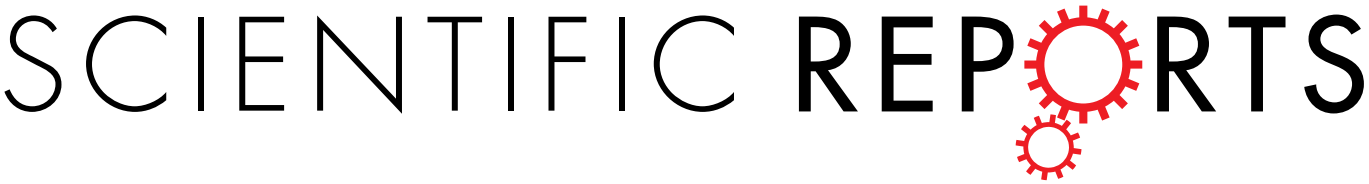

OPEN

Classical-to-quantum transition behavior between two oscillators separated in space under the action of optomechanical interaction

Received: 19 October 2016
Accepted: 21 April 2017
Published online: 31 May 2017

Cheng-Hua Bai, Dong-Yang Wang, Hong-Fu Wang, Ai-Dong Zhu & Shou Zhang

We propose a scheme to show that the system consisting of two macroscopic oscillators separated in space which are coupled through Coulomb interaction displays the classical-to-quantum transition behavior under the action of optomechanical coupling interaction. Once the optomechanical coupling interaction disappears, the entanglement between the two separated oscillators disappears accordingly and the system will return to classical world even though there exists sufficiently strong Coulomb coupling between the oscillators. In addition, resorting to the squeezing of the cavity field generated by an optical parametric amplifier inside the cavity, we discuss the effect of squeezed light driving on this classical-to-quantum transition behavior instead of injecting the squeezed field directly. The results of numerical simulation show that the present scheme is feasible and practical and has stronger robustness against the environment temperature compared with previous schemes in current experimentally feasible regimes. The scheme might possibly help us to further clarify and grasp the classical-quantum boundary.

Quantum entanglement[1,2], a most remarkable feature and a cornerstone of quantum physics, plays a significant role in the foundation of quantum theory and also has potential applications in quantum technology, such as quantum information science[3] and quantum metrology[4]. So far, one has had a fairly good understanding of how to generate entanglement among microscopic entities and entanglement has been successfully prepared and manipulated in variously microscopic systems theoretically and experimentally, such as atoms[5–9], photons[10–12], ions[13–15], Bose-Einstein condensates[16], and so on. However, it is not yet completely clear that to what degree quantum mechanics is suitable for mesoscopic and macroscopic systems and the generation of quantum entanglement of mesoscopic or macroscopic bodies in mechanical motion is generally bounded by the thermal fluctuation exerted by their environments. Recently, there has been considerable interest in investigating entanglement in mesoscopic and even macroscopic systems[17–28]. This is due to the fact that such entanglement might provide explicit evidence for quantum phenomena[29] and even might possibly help us to clarify the classical-to-quantum transition, as well as the boundary between classical and quantum worlds[30]. Since mechanical oscillators resemble a prototype of classical systems, they are beginning to be important candidates for the investigation of quantum features at mesoscopic and macroscopic scales. Additionally, with the rapid progress of practical technologies in cavity optomechanics, the mechanical oscillators can be cooled down close to the quantum ground state[31–33]. Thus they provide a nature platform to explore non-classical effects in macroscopic systems[34,35].

In recent years, based on the optomechanical systems, some schemes have been brought forward to generate entanglement between macroscopic oscillators from many different angles of view: such as entangling two oscillators in a ring cavity[17,18], entangling two distantly separated oscillators by utilizing the entangled light fields[19], entangling two oscillators via a double-cavity set-up by driving squeezing optical fields[20], entangling a Fabry-Pérot cavity's two moving mirrors by driving an intense classical laser field[21], entangling two dielectric membranes suspended inside a Fabry-Pérot cavity[22], entangling two macroscopic mechanical resonators induced by the radiation pressure of a single photon in a two-cavity optomechanical system[23], generating steady-state entanglement of remote mechanical oscillators in unidirectionally coupled cavities by the cascaded cavity coupling[24], realizing entanglement of spatially separated mechanical modes via applying a bichromatic pump leads

Department of Physics, College of Science, Yanbian University, Yanji, Jilin, 133002, China. Correspondence and requests for materials should be addressed to H.-F.W. (email: hfwang@ybu.edu.cn)

to time-dependent optical springs that can tune couplings between nondegenerate mechanical modes into the type of parametric amplifier resonance[25], generating entanglement between two mechanical resonators with different frequencies either dynamically or in the steady state[26], and entangling two movable mirrors in an optomechanical cavity in which a Kerr-down-conversion crystal consisting of a Kerr nonlinear medium and an optical parametric amplifier (OPA) is placed[27]. In these schemes, we can roughly classify these mechanical entanglement state-generation schemes into two categories, according to the entanglement is created by purely optomechanical means[17,22–26], or is adjusted by the squeezed field[18–21,27]. Huang and Agarwal proposed a scheme to entangle two separated mechanical oscillators by injecting broad band squeezed vacuum light and laser light into the ring cavity[18]. This scheme showed that the entanglement can be modulated via the squeezing parameter of the input light. In the case of no injection of the squeezed vacuum light, which means that the squeezed vacuum light is replaced by the ordinary vacuum light, there is always no entanglement between the separated oscillators. However, once the incident vacuum light is squeezed, the entanglement exists. Pinard *et al*. also proposed a scheme to generate a stationary entangled state of two movable mirrors if and only if the incident fields are squeezed[20]. In ref. 27 even though the entanglement between two mechanical oscillators in an optomechanical cavity can be generated when the injected field is not squeezed, the region of entanglement is discrete and very narrow, so which inevitably brings difficulties to achieve the entanglement in experiment. However, when the injected field is adjusted to the squeezed field, the region of entanglement is continuous and greatly enlarged. In essence, the OPA inside the optomechanical cavity can produce various novel effects including improvement of the cooling of the micromechanical mirror[36], affection of the normal-mode splitting behavior of the coupled movable mirror and the cavity field[37], achievement of strong mechanical squeezing[38], and enhancement of the precision of optomechanical position detection[39]. The nonlinear interaction processes between light and OPA have been demonstrated as important sources of squeezed state of the radiation field[40,41]. In 2016, Agarwal and Huang have had the OPA placed inside the optomechanical cavity so that the squeezing cavity field is generated inside the cavity[38]. Via driving the system by the red-detuned laser in the resolved sideband limit makes the optomechanical interaction between the movable mirror and the cavity field like a beam-splitter interaction, the state of squeezed photons transfers to phonons with almost 100% efficiency, the strong mechanical squeezing is thus achieved.

Recently, the hybrid quantum system consisting of two coupled resonators has been investigated[42,43]. Here we propose a scheme to show that the system consisting of two macroscopic oscillators separated in space which are coupled through Coulomb interaction displays the classical-to-quantum transition behavior under the auxiliary of the optomechanical coupling interaction. Our investigation indicates that once the optomechanical coupling interaction disappears, the entanglement between the two separated oscillators disappears accordingly and the system will return to classical world even though there exists sufficiently strong Coulomb coupling between the oscillators. Resorting to the squeezing of the cavity field generated by an OPA inside the cavity, we discuss the effect of squeezed light driving on this classical-to-quantum transition behavior instead of injecting the squeezed field directly. In current experimentally feasible regimes, the results of numerical simulation show that the present scheme is feasible and practical and has stronger robustness against the environment temperature compared with previous schemes. It is promising that the scheme might possibly help us to further clarify and grasp the classical-quantum boundary.

The paper is organized as follows. In Sec. 2, we describe the model and present the quantum Langevin equations. In Sec. 3, we present the definition of the covariance matrix and transform the quantum Langevin equations into a equivalent differential equation of the covariance matrix. In Sec. 4, we show that the system consisting of two macroscopic oscillators separated in space which are coupled through Coulomb interaction displays the classical-to-quantum transition behavior under the auxiliary of optomechanical coupling interaction and discuss the effect of squeezed light driving generated by the OPA inside the cavity on this classical-to-quantum transition behavior in current experimentally feasible steady regime. Finally we make a conclusion to summarize our results in Sec. 5.

Results

Model and equations of motion. The system considered consists of a Fabry-Pérot cavity containing one fixed partially transmitting mirror A and one movable totally reflecting mirror B_1 in contact with a thermal bath in equilibrium at temperature T, a charged oscillator B_2, and an OPA which is embedded into the cavity, as schematically shown in Fig. 1. The movable mirror B_1 can move along the cavity axis and is treated as a mechanical harmonic oscillator with effective mass m, frequency ω_1, and energy decay rate γ_{m_1} and is charged by the bias gate voltage U_1. The cavity mode couples to the mechanical oscillator B_1 via radiation pressure caused by the intracavity photons exerting on the movable mirror, while B_1 and B_2 are coupled by the Coulomb force[44–47]. The cavity is coherently driven by an external laser with frequency ω_L and amplitude E from left side. The Hamiltonian of the system is given by

$$\begin{aligned} H &= \hbar\omega_c c^\dagger c + \frac{\hbar\omega_{m1}}{2}(p_1^2+q_1^2) + \frac{\hbar\omega_{m2}}{2}(p_2^2+q_2^2) + i\hbar E(c^\dagger e^{-i\omega_L t} - ce^{i\omega_L t}) \\ &\quad - \hbar G_0 c^\dagger c q_1 + i\hbar C_g(e^{i\theta}c^{\dagger 2}e^{-2i\omega_L t} - e^{-i\theta}c^2 e^{2i\omega_L t}) + \frac{-k_e Q_{C1}Q_{C2}}{|d_0+Q_1-Q_2|}, \end{aligned} \tag{1}$$

where the first term is the free Hamiltonian for the cavity field with resonance frequency ω_c and annihilation (creation) operator c ($c^\dagger$). The second and third terms describe the vibration of the mechanical oscillators B_1 and B_2, respectively, and the dimensionless position operator $q_j = \frac{1}{\sqrt{2}}\frac{Q_j}{x_{zp}}$ and momentum operator $p_j = \frac{1}{\sqrt{2}}\frac{P_j}{p_{zp}}$ satisfy the commutation relation $[q_j, p_j] = i$ ($j = 1, 2$), where x_{zp} and p_{zp} are, respectively, the stand deviation of the zero-point motion and zero-point momentum of the oscillator. The fourth term is the pumping interaction

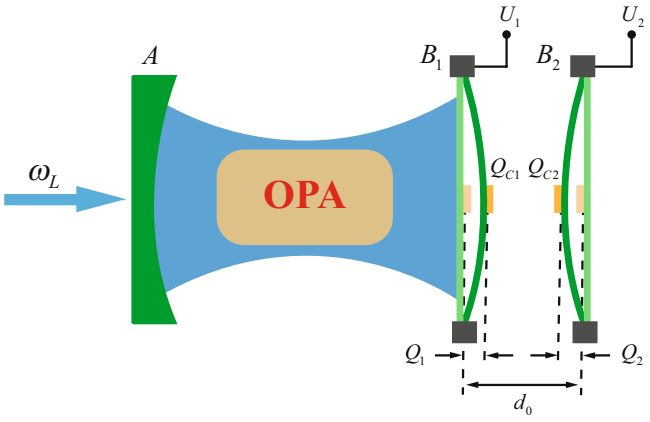

Figure 1. Schematic diagram of the system. The cavity optomechanical system consists of a fixed mirror A and a mechanical oscillator B_1 which is coupled to the other mechanical oscillator B_2 under the action of the Coulomb interaction. An OPA is placed inside the cavity, and the pump of the OPA is not shown. The cavity is driven by the driving field E with frequency ω_L. The electrode carrying charge Q_{C1} (Q_{C2}) on B_1 (B_2) is charged by the bias gate voltage U_1 (U_2). d_0 is equilibrium separation of B_1 and B_2. Q_1 and Q_2 are the small deviation of B_1 and B_2 from their equilibrium positions, respectively, due to the radiation pressure interaction and Coulomb interaction.

between the cavity field and external deriving laser with $E = \sqrt{2\kappa P/\hbar\omega_L}$, where P is the power of the driving laser and κ is the cavity decay rate. The fifth term describes the optomechanical interaction between the cavity field and the mechanical oscillator B_1 with the optomechanical coupling strength $G_0 = (\omega_c/L)\sqrt{\hbar/m\omega_{m1}}$, where L is the separation between the mirror A and oscillator B_1 in the absence of radiation pressure and Coulomb interactions. The sixth term represents the coupling between the OPA and the cavity field, where C_g is the nonlinear gain of the OPA and θ is the phase of the pump driving the OPA, i.e., the phase shift between the signal (idler) mode and the pump mode. The last term represents the Coulomb interaction of the two charged mechanical oscillators B_1 and B_2. k_e denotes the electrostatic constant. $Q_{Cj} = C_jU_j$ is the charge carried by the electrode on oscillator B_j, where C_j is the capacitance of the bias gate on B_j. d_0 is the equilibrium separation between B_1 and B_2 in the absence of optomechanical and Coulomb interactions and Q_j represents the small deviation of B_j from its equilibrium position due to the optomechanical and Coulomb interactions.

Since the mechanical deviation Q_j is comparatively small compared to the equilibrium separation d_0, i.e., $Q_j \ll d_0$, the term of Coulomb interaction can be expanded to second-order of $(Q_1 - Q_2)/d_0$ as follows

$$H_{\mathrm{CI}} = \frac{-k_eC_1U_1C_2U_2}{|d_0 + Q_1 - Q_2|} = \frac{-k_eC_1U_1C_2U_2}{d_0}\left[1 - \frac{Q_1 - Q_2}{d_0} + \left(\frac{Q_1 - Q_2}{d_0}\right)^2\right], \tag{2}$$

where the linear term can be neglected via redefining the equilibrium positions of mechanical oscillators and the quadratic term includes a renormalization of the mechanical frequencies for both B_1 and B_2. Through further discarding the constant term, the Coulomb interaction can be reduced to the simpler form

$$H_{\mathrm{CI}} = \hbar\lambda q_1q_2, \tag{3}$$

where $\lambda = 2k_eC_1U_1C_2U_2/m\omega_m d_0^3$[44,46–48]. In the interaction picture with respect to $\hbar\omega_Lc^\dagger c$, the system Hamiltonian can be rewritten as

$$\begin{aligned} H &= \hbar(\omega_c - \omega_L)c^\dagger c + \frac{\hbar\omega_{m1}}{2}(p_1^2 + q_1^2) + \frac{\hbar\omega_{m2}}{2}(p_2^2 + q_2^2) + \hbar\lambda q_1q_2 \\ &\quad + i\hbar E(c^\dagger - c) - \hbar G_0c^\dagger cq_1 + i\hbar C_g(e^{i\theta}c^{\dagger 2} - e^{-i\theta}c^2). \end{aligned} \tag{4}$$

A proper analysis of the system must consider the photon losses from the cavity and the Brownian noise from the environment. This can be accomplished via the dynamics of the system governed by Eq. (4) using quantum Langevin equation

$$\begin{aligned} \dot{q}_1 &= \omega_{m1}p_1, \\ \dot{p}_1 &= -\omega_{m1}q_1 - \gamma_{m1}p_1 + G_0c^\dagger c - \lambda q_2 + \xi_1, \\ \dot{q}_2 &= \omega_{m2}p_2, \\ \dot{p}_2 &= -\omega_{m2}q_2 - \gamma_{m2}p_2 - \lambda q_1 + \xi_2, \\ \dot{c} &= -[\kappa + i(\omega_c - \omega_L)]c + iG_0cq_1 + E + 2C_ge^{i\theta}c^\dagger + \sqrt{2\kappa}\,c_{in}, \end{aligned} \tag{5}$$

where γ_{m2} is the damping rate for the oscillator B_2. c_{in} is the input vacuum noise operator with zero mean value and nonzero correlation function $\langle c_{in}(t)c_{in}^{\dagger}(t')\rangle = \delta(t-t')$[19,49,50]. The quantum Brownian noise $\xi_1(\xi_2)$ arises from the coupling between B_1 (B_2) and its environment with zero mean value and correlation function[51]

$$\langle \xi_j(t)\xi_j(t')\rangle = \frac{\gamma_{mj}}{\omega_{mj}}\int \frac{\omega}{2\pi} e^{-i\omega(t-t')}\left[\coth(\frac{\hbar\omega}{2k_BT}) + 1\right]d\omega, \tag{6}$$

where k_B is the Boltzmann constant and T is the temperature of the environment in contact with the oscillators. However, quantum effects are revealed just for the oscillators with a large quality factor, i.e., $Q \gg 1$. In this limit, Eq. (6) can be further simplified to delta-correlated[51]

$$\langle \xi_j(t)\xi_j(t') + \xi_j(t')\xi_j(t)\rangle/2 \simeq \gamma_{mj}(2\bar{n}+1)\delta(t-t'), \tag{7}$$

where $\bar{n} = (\exp\{\hbar\omega_{mj}/k_BT\} - 1)^{-1}$ is the mean thermal excitation number. In the following we present the definition of the covariance matrix and transform the Langevin equations into a equivalent differential equation of the covariance matrix.

Equation of motion for covariance matrix. The stability of the steady state of the system is determined by a linearized analysis for small perturbation around the steady state[41]. We now first linearize the dynamics of the system. The nonlinear quantum Langevin equations can be linearized via rewriting each Hersenberg operator as its steady state mean-value plus an additional fluctuation operator with zero-mean value, i.e., $q_j = q_{js} + \delta q_j$, $p_j = p_{js} + \delta p_j$, and $c = c_j + \delta c$[52]. After inserting these expressions into the Langevin equations of Eq. (5), we can obtain a set of nonlinear algebraic equations for the steady state values and a set of quantum Langevin equations for the fluctuation operators[53]. Through setting all the time derivatives in algebra equations for the steady state value to zero, the steady state mean values of system are given by

$$\begin{aligned} p_{1s} &= 0, \\ q_{1s} &= \frac{G_0|c_s|^2}{\omega_{m1} - \frac{\lambda^2}{\omega_{m2}}}, \\ p_{2s} &= 0, \\ q_{2s} &= \frac{-\lambda}{\omega_{m2}} q_{1s}, \\ c_s &= \frac{\kappa - i\Delta + 2C_g e^{i\theta}}{\kappa^2 + \Delta^2 - 4C_g^2} E, \end{aligned} \tag{8}$$

where $\Delta = \omega_c - \omega_L - G_0 q_{1s}$ is the effective cavity detuning from the frequency of the input laser in the presence of the radiation pressure. The modification of the detuning by the $G_0 q_{1s}$ term depends on the mechanical motion. The q_{1s} represents the new equilibrium position of the oscillator B_1 relative to that in the absence of the optomechanical and Coulomb interactions and c_s denotes the steady state amplitude of the cavity field.

In order to analyze the oscillator-oscillator steady state entanglement, we need to find out the fluctuations in the oscillators' amplitudes. So we are interested in the dynamics of small fluctuations around the steady state of the system. For generating the entanglement, generally, the cavity is intensively driven with a very large input power P, which means that at the steady state, the intracavity field has a large amplitude, i.e., $|c_s| \gg 1$. In this strong driving limit, we can ignore some small quantities and get the linearized Langevin equations

$$\begin{aligned} \delta\dot{q}_1 &= \omega_{m1}\delta p_1, \\ \delta\dot{p}_1 &= -\omega_{m1}\delta q_1 - \gamma_{m1}\delta p_1 - \lambda\delta q_2 + G_0(c_s^*\delta c + c_s\delta c^{\dagger}) + \xi_1, \\ \delta\dot{q}_2 &= \omega_{m2}\delta p_2, \\ \delta\dot{p}_2 &= -\lambda\delta q_1 - \omega_{m2}\delta q_2 - \gamma_{m2}\delta p_2 + \xi_2, \\ \delta\dot{c} &= -(\kappa + i\Delta)\delta c + iG_0 c_s\delta q_1 + 2C_g e^{i\theta}\delta c^{\dagger} + \sqrt{2\kappa}\, c_{in}. \end{aligned} \tag{9}$$

If we choose the phase reference of the cavity field so that c_s is real via adjusting the phase of the driving laser to $\arctan\left[\frac{\Delta - 2C_g\sin\theta}{\kappa + 2C_g\cos\theta}\right]$ and introduce the amplitude and phase fluctuations of the cavity field as $\delta X = (\delta c + \delta c^{\dagger})/\sqrt{2}$ and $\delta Y = (\delta c - \delta c^{\dagger})/\sqrt{2}\,i$, and the position and momentum fluctuations of the thermal noise as $X^{in} = (c_{in} + c_{in}^{\dagger})/\sqrt{2}$ and $Y^{in} = (c_{in} - c_{in}^{\dagger})/\sqrt{2}\,i$, Eq. (9) can be written as the matrix form

$$\dot{f}(t) = Mf(t) + \eta(t), \tag{10}$$

where $f(t)$ is the column vector of the fluctuations and $\eta(t)$ is the column vector of the noise sources. Their transposes are

$$f(t)^T = (\delta q_1, \delta p_1, \delta q_2, \delta p_2, \delta X, \delta Y),\ \eta(t)^T = (0, \xi_1, 0, \xi_2, \sqrt{2\kappa}X^{in}, \sqrt{2\kappa}Y^{in}); \tag{11}$$

and the matrix M is given by

$$M=\begin{bmatrix} 0 & \omega_{m1} & 0 & 0 & 0 & 0 \\ -\omega_{m1} & -\gamma_{m1} & -\lambda & 0 & G_m & 0 \\ 0 & 0 & 0 & \omega_{m2} & 0 & 0 \\ -\lambda & 0 & -\omega_{m2} & -\gamma_{m2} & 0 & 0 \\ 0 & 0 & 0 & 0 & 2C_g\cos\theta-\kappa & 2C_g\sin\theta+\Delta \\ G_m & 0 & 0 & 0 & 2C_g\sin\theta-\Delta & -(2C_g\cos\theta+\kappa) \end{bmatrix}, \tag{12}$$

where $G_m=\sqrt{2}G_0c_s$ is the effective optomechanical coupling. Remarkably, the quantum fluctuations of the field and the oscillator are now coupled by the much large effective coupling.

The solutions to Eq. (10) are stable only if all the eigenvalues of the matrix M have negative real parts. The stability conditions can be derived by applying the Routh-Hurwitz criterion[54,55], yielding the constrain conditions on the system parameters. Due to their expressions are considerable tedious, we don't report them here. However, we will satisfy the stability conditions of the system in the following analysis.

The solution of the first-order linear inhomogeneous differential Eq. (10) can be solved as following form

$$f(t)=u(t)f(0)+\int_0^t u(\tau)\eta(t-\tau)d\tau, \tag{13}$$

where the matrix $u(t)=\exp(Mt)$ and the initial condition $u(0)=I$ (I is the identity matrix).

An important type of continuous variable quantum states is the Gaussian states, which play a significant role in the foundation of quantum theory and also have potential applications in their relevant experiment[56]. The linearized effective Hamiltonian which corresponds to the linearized Langevin Eq. (9) ensures that when the system is stable, it always reaches a Gaussian state whose information-related properties, such as entanglement and entropy, can be completely described by the symmetric 6×6 covariance matrix V[56,57] with components defined as

$$V_{i,j}=\langle f_if_j+f_jf_i\rangle/2. \tag{14}$$

From Eqs (10) and (14), we can derive a linear differential equation for the covariance matrix

$$\dot{V}=MV+VM^T+D, \tag{15}$$

where D is a diffusion matrix whose components are associated with the noise correlation function Eq. (7)

$$D_{i,j}\delta(t-t')=\langle\eta_i(t)\eta_j(t')+\eta_j(t')\eta_i(t)\rangle/2. \tag{16}$$

It is easy to obtain that D is diagonal $D=\mathrm{diag}[0,\ \gamma_{m1}(2\bar{n}+1),\ 0,\ \gamma_{m2}(2\bar{n}+1),\ \kappa,\ \kappa]$. From the point of view of describing the dynamics of the system Gaussian states, Eq. (15) is equivalent to the quantum Langevin equations Eq. (9) but is more convenient for studying entanglement evolution.

The reduced 4×4 covariance matrix $\widetilde{V}$ for the mechanical oscillators B_1 and B_2 of interest here can be extracted from the full 6×6 covariance matrix V. If the reduced covariance matrix $\widetilde{V}$ is written as the block form

$$\widetilde{V}=\begin{bmatrix}\Phi_1 & \Phi_3\\ \Phi_3^T & \Phi_2\end{bmatrix}, \tag{17}$$

where $\Phi_k(k=1,2,3)$ are 2×2 block matrices, then the entanglement of the two separated mechanical oscillators B_1 and B_2 quantified by the logarithmic negativity can be readily calculated[58–60]

$$E_N=\max[0,-\ln(2\rho)], \tag{18}$$

where $\rho\equiv2^{-1/2}\{\Sigma(V)-[\Sigma(V)^2-4\det V]^{1/2}\}^{1/2}$, with $\Sigma(V)\equiv\det\Phi_1+\det\Phi_2-2\det\Phi_3$. Therefore, a Gaussian state is entangled if and only if $\rho<1/2$, which is equivalent to Simon's necessary and sufficient entanglement nonpositive partial transpose criterion for Gaussian states[61].

The classical-to-quantum transition behavior between two oscillators separated in space in the steady regime. In this section, we will show that the system consisting of two oscillators separated in space which are coupled through Coulomb interaction displays the classical-to-quantum transition behavior under the action of optomechanical coupling interaction and discuss the effect of squeezed light driving generated by the OPA inside the cavity on this classical-to-quantum transition behavior via numerically evaluating the logarithmic negativity E_N in current experimentally feasible steady regime. Here, we assume that all the parameters of the two mechanical oscillators to be the same, i.e., $\omega_{m1}=\omega_{m2}=\omega_m$, $\gamma_{m1}=\gamma_{m2}=\gamma_m$. We choose the parameters in our numerical calculations are based on the experiment conditions[62,63]: $\omega_m=200\pi$ MHz, $\gamma_m=200\pi$ Hz, $\kappa=88.1$ MHz, $m=5$ ng, $L=1$ mm, and the wavelength of driving laser $\lambda_0=810$ nm.

First, we illustrate the effect of the Coulomb interaction on the entanglement between the two separated mechanical oscillators in the absence of the OPA ($C_g=0$), i,e., ordinary light driving. The logarithmic negativity E_N as a function of the normalized detuning Δ/ω_m for three different values of the Coulomb coupling strength $\lambda=0.3\,\omega_m$ (orange diamond line), $\lambda=0.5\,\omega_m$ (blue square line), and $\lambda=0.95\,\omega_m$ (red sphere line) at temperature $T=4$ mK and driving power $P=50$ mW in the absence of the OPA is shown in Fig. 2(a). As illustrated in previous

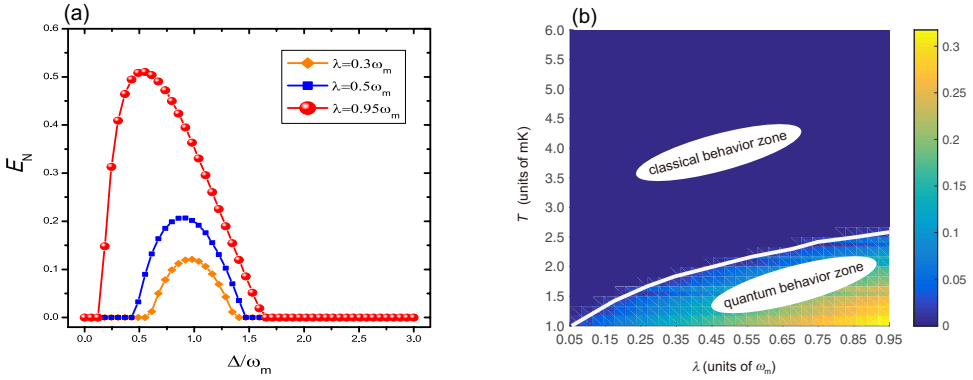

Figure 2. (**a**) Plot of the logarithmic negativity E_N as a function of the normalized detuning Δ/ω_m for three different values of the Coulomb coupling strength $\lambda = 0.3\,\omega_m$ (orange diamond line), $\lambda = 0.5\,\omega_m$ (blue square line), and $\lambda = 0.95\,\omega_m$ (red sphere line) in the absence of the OPA ($C_g = 0$). Here the temperature of environment and driving power are set to $T = 4$ mK and $P = 50$ mW, respectively. (**b**) The logarithmic negativity E_N versus the environment temperature T and the Coulomb coupling strength λ in the absence of the optomechanical coupling between the optical field and the oscillator B_1, i.e., $G_0 = 0$. The rest parameters are chosen as $\omega_m = 200\,\pi$MHz and $\gamma_m = 200\,\pi$Hz.

section, as long as the logarithmic negativity $E_N > 0$, the entanglement exists between the two oscillators, meaning that there is a quantum correlation between them, even though they are separated in space. From Fig. 2(a), one can clearly see that the larger the coupling parameter λ is, the stronger the oscillators entangle and the broader the range of the entanglement is. The numerical result shows that if there is no the Coulomb coupling, it is not possible to entangle the two oscillators which are separated in space. Now, we consider the feasibility of the choice of numerical value of the coupling strength λ in experiment. If we apply the reported experimental parameters, i.e., the capacitance of the bias gate on B_1 and B_2 $C_1 = C_2 = 2.4$ nF, the equilibrium distance between B_1 and B_2 without optomechanical and Coulomb interactions $d_0 = 160\,\mu$m[47], and adjust the bias gate voltage $U_1 = U_2 = 200$ V, in this case, $\lambda \simeq 0.33\,\omega_m$. Compared with the numerical value needed in our scheme, it has the same order of magnitude, so the choice of the numerical value of λ is feasible in experiment.

Subsequently, we consider the role of the optomechanical coupling between the optical field and the oscillator B_1 plays in the generating entanglement between two separated oscillators in space. For this purpose, we make a density plot of E_N versus the environment temperature T and the Coulomb coupling strength λ in the absence of the optomechanical coupling, i.e., $G_0 = 0$, in Fig. 2(b). As shown in Fig. 2(b), it can be clearly seen that in the case of absence of optomechanical coupling, if we decrease the environment temperature T to the range of quite low and the Coulomb coupling strength λ is quite strong, the system consisting of two separated oscillators in space will display the quantum entanglement behavior. But with the increase of temperature, the quantum entanglement behavior will disappear and the system returns to classical world, even though there exists the sufficiently strong Coulomb coupling between the two oscillators. This is the reason why we can not observe the quantum phenomena in macroscopic world generally. The higher the environment temperature is, the stronger the thermal noise is. Then the entanglement between the two separated oscillators in space is submerged by the strong thermal noise. So the generation of quantum entanglement of mesoscopic or macroscopic bodies in mechanical motion is generally bounded by the thermal noise exerted by their environments. However, under the auxiliary of the optomechanical coupling, the two separated oscillators in space in the classical behavior zone can display the quantum entanglement behavior. From Fig. 2, it can be clearly seen that once the optomechanical coupling between the optical field and oscillator B_1 disappears, the entanglement between the two separated oscillators in space will disappear accordingly and the system returns to classical world. This is due to the optomechanical coupling between the optical field and oscillator cools down the oscillator and sufficiently suppresses the detrimental effect of the thermal noise. Hence, the optomechanical coupling between the optical mode and the mechanical mode provides a perfect platform for the study of this classical-to-quantum transition behavior.

In the previous schemes, ref. 18 proposed a method to entangle two separated oscillators by injecting squeezed vacuum light and laser light into the ring cavity. The entanglement between the oscillators can be modulated via the squeezing parameter of the input light. When the squeezed vacuum light is replaced by an ordinary vacuum light, i.e., the squeezing parameter of the input light is 0, there is no entanglement between the oscillators. However, on squeezing the injected vacuum light, the entanglement between the oscillators is emerged. When the squeezing parameter of the input light $r \in (0, 1)$, the entanglement becomes more and more stronger with the increase of r, while for $r \in (1, 2)$, the entanglement becomes more and more weaker with the increase of r. So in this scheme the entanglement between the separated oscillators is affected by the driven light is squeezed or not to a large extent. Ref. 27 also proposed to coherently control the entanglement between two movable mirrors via placing the Kerr-down-conversion crystal consisting of Kerr nonlinear medium and OPA inside an optomechanical cavity. By the aid of the input squeezed vacuum field, the Kerr nonlinear medium can lead to stronger entanglement between the two movable mirrors and extend to wider entanglement region. Whereas the effect of the OPA on entanglement is completely opposite, it leads weaker entanglement and narrower entanglement region.

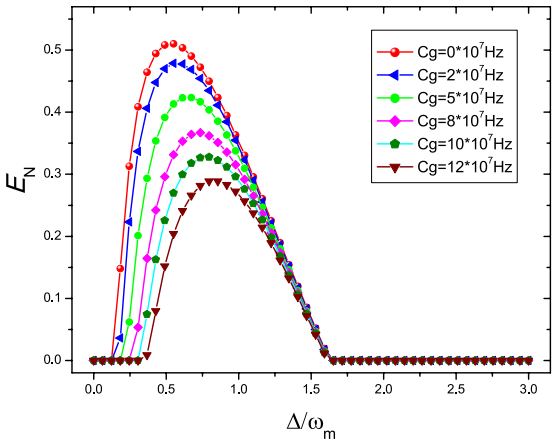

Figure 3. Plot of the logarithmic negativity E_N as a function of the normalized detuning Δ/ω_m for six different values of $C_g = 0$ (red sphere line), $C_g = 2 \times 10^7$ Hz (blue triangle line), $C_g = 5 \times 10^7$ Hz (green circle line), $C_g = 8 \times 10^7$ Hz (magenta diamond line), $C_g = 10 \times 10^7$ Hz (olive pentagon line), and $C_g = 12 \times 10^7$ Hz (wine triangle line). Here we set the Coulomb coupling strength $\lambda = 0.95\,\omega_m$, the phase of the pump driving $\theta = 0$, the temperature of environment $T = 4$ mK, and the laser driving power $P = 50$ mW.

Likewise, the entanglement between two separated movable mirrors is remarkably affected by the input squeezed field. The above two schemes have the common point that they all resort to the external squeezed vacuum filed and are dependent in a important way on the driving of squeezed light. So a natural curiosity and question are that whether the driving of squeezed light will affect this classical-to-quantum transition behavior of the system consisting of two macroscopic oscillators separated in space or not and how to affect. As we all know, the nonlinear interaction processes between light and OPA have been considered as important sources of squeezed state of the radiation field[40,41]. Fortunately, in 2016, Agarwal and Huang investigated the dependence of the amount of squeezing of the intracavity photons on the parametric gain and driving phase of an OPA[38]. Next, resorting to the squeezing of the cavity field generated by an OPA inside the cavity, we discuss the effect of squeezed light driving on this classical-to-quantum transition behavior instead of injecting the squeezed field directly.

We now show the effect of the gain of the OPA C_g on the entanglement between the oscillators. We fix the Coulomb coupling strength $\lambda = 0.95\,\omega_m$, the phase of the pump driving $\theta = 0$, the temperature of environment $T = 4$ mK, and the laser driving power $P = 50$ mW. The logarithmic negativity E_N as a function of the normalized detuning Δ/ω_m for six different values of $C_g = 0$ (red sphere line), $C_g = 2 \times 10^7$ Hz (blue triangle line), $C_g = 5 \times 10^7$ Hz (green circle line), $C_g = 8 \times 10^7$ Hz (magenta diamond line), $C_g = 10 \times 10^7$ Hz (olive pentagon line), and $C_g = 12 \times 10^7$ Hz (wine triangle line) is shown in Fig. 3. From Fig. 3, we can find that the entanglement between the oscillators becomes more and more weaker and the entanglement region becomes more and more narrower with the increase of the gain of the OPA C_g compared with the case of in the absence of OPA ($C_g = 0$). This is because increasing the parametric gain C_g would lead to larger amount of squeezing of the cavity field when the phase of the pump driving is set to $\theta = 0$[38]. As we all know, the radiation pressure exerted on the oscillator B_1 by the cavity field depends on the number operator and then it is sensitive to the photon statistics of the intracavity field. The photon statistics can be calculated from the quantum Langevin Eq. (9). It can be proved that the Wigner function W of the intracavity field is Gaussian of the form $\exp[\mu(\alpha - c_s)^2 + \nu(\alpha^* - c_s^*)^2 + \eta(\alpha - c_s)(\alpha^* - c_s^*)]$, with μ, ν, η determined by κ, Δ, C_g, θ, etc. The photon number distribution associated with such a Gaussian Wigner function depends in an important way on the parameter μ and the inequality of μ and ν[64] and the latter depend on $C_g \neq 0$ or the presence of OPA in the cavity. The parametric squeezing processes inside the cavity change the quantum statistics of the field and larger amount of squeezing increases the photon number in the cavity, which lead to a stronger radiation pressure acting on the oscillator B_1. However, besides the radiation pressure, there is another interaction, i.e., Coulomb coupling with the oscillator B_2, acts on the oscillator B_1 simultaneously. As to the oscillator B_1, there exists the competing effect between the radiation pressure interaction and Coulomb interaction. So increasing the parametric gain C_g corresponds to a stronger radiation pressure, which seems to be equivalent to decrease the Coulomb coupling strength between the two separated oscillators in space in the absence of OPA ($C_g = 0$), as shown in Fig. 2(a). Additionally, the position of the maximal entanglement moves to right with the increase of gain C_g due to the fact that the injection of OPA strengths the steady intracavity field and in turn changes the effective deduning Δ. This is very similar to such the case of the weaker Coulomb coupling strength in the absence of OPA as shown in Fig. 2(a).

We next examine the effect of the phase of the pump driving the OPA θ on the entanglement between the oscillators. We fix the gain of the OPA $C_g = 12 \times 10^7$ Hz and other parameters are as same as the Fig. 3. The logarithmic negativity E_N as a function of the normalized detuning Δ/ω_m for four different values of the phase of the pump driving the OPA $\theta = 0$ (olive diamond line), $\theta = \pi/16$ (blue pentagon line), $\theta = \pi/6$ (green triangle line), and $\theta = \pi/4$ (red sphere line) is shown in Fig. 4. It can be clearly seen that the entanglement between the oscillators becomes more and more stronger with the increase of the phase θ when $\Delta < \omega_m$ for the fixed gain C_g of the OPA. This is due to the fact that increasing the phase of the pump driving θ corresponds to a smaller amount of

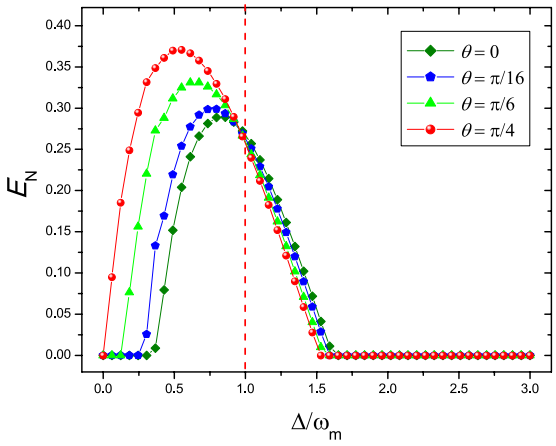

Figure 4. Plot of the logarithmic negativity E_N as a function of the normalized detuning Δ/ω_m for four different values of the phase of the pump driving the OPA $\theta = 0$ (olive diamond line), $\theta = \pi/16$ (blue pentagon line), $\theta = \pi/6$ (green triangle line), and $\theta = \pi/4$ (red sphere line). Here we set the Coulomb coupling strength $\lambda = 0.95\,\omega_m$, the gain of the OPA $C_g = 12 \times 10^7$ Hz, the temperature of environment $T = 4$ mK, and the laser driving power $P = 50$ mW.

squeezing of the cavity field[38] and the Coulomb interaction becomes the dominant factor compared with the radiation pressure interaction for the oscillator B_1. So the influence of phase driving θ on the entanglement between the two separated oscillators in space is completely opposite compared with the function of the parametric gain C_g as shown in Fig. 3. We can also find that when $\Delta = \omega_m$, all curves are intersected in one point. This can be interpreted as driving the system by the red-detuned laser $\Delta = \omega_m$ in the resolved sideband limit makes the optomechanical interaction between the cavity field and the oscillator B_1 like a beam-splitter interaction. In such case, the competing effect between the radiation pressure interaction and the Coulomb interaction acting on the oscillator B_1 maintains a balance.

Hence, resorting to the squeezing of the cavity field generated by an OPA inside the cavity, we successfully analyze the effect of squeezed light driving on this classical-to-quantum transition behavior instead of injecting the squeezed field directly. In the following, we show the effect of the Brownian noise on the entanglement between the oscillators, i.e., the effect of the temperature of the environment. The logarithmic negativity E_N as a function of the temperature for four different values of the laser power $P = 30$ mW (dark yellow triangle line), $P = 50$ mW (purple pentagon line), $P = 80$ mW (green diamond line), and $P = 100$ mW (red sphere line) when the Coulomb coupling strength $\lambda = 0.95\,\omega_m$, $\Delta = 0.75\,\omega_m$, and the phase of the pump driving $\theta = \pi/16$ is plotted in Fig. 5, where C_g is set as 0, 2×10^7 Hz, 8×10^7 Hz, and 12×10^7 Hz, respectively. It can be concluded that for the fixed gain C_g of the OPA, as the temperature of the environment increases, the amount of entanglement monotonically decreases due to the environment thermal noise induced decoherence which is as expected. The higher the temperature of the environment is, the stronger the thermal noise is. Then the entanglement between two oscillators is submerged by the strong thermal noise. The critical temperature of the entanglement is improved with the increase of the laser driving power for the fixed gain C_g of the OPA and the numerical simulation results indicate that the robustness is obviously increased compared with previous schemes[18,27]. While for the fixed laser driving power, the critical temperature of the entanglement is higher with respect to the larger gain C_g of the OPA. More importantly, from Fig. 5(a,d), it is remarkable that compared with the case of absence of the OPA, the presence of OPA obviously increases the robustness against the environment temperature of this classical-to-quantum transition behavior between the oscillators separated in space. It has also been verified that the OPA inside a cavity can considerably improve the cooling of the oscillator by radiation pressure[36]. Additionally, the relevant experimental investigation in such temperature requirement can be explored in the circuit cavity electromechanics[65], which is easily cooled to the temperature below 100 mK.

In practice, it is hard to achieve two totally identical oscillators in experiment. So it is greatly necessary to consider the case in which the two separated oscillators in space have different frequencies ($\omega_{m1} \neq \omega_{m2}$). For this reason, we plot the logarithmic negativity E_N when the two oscillators have different frequencies in Fig. 6, where we set $\omega_{m1} = \omega_m$, $\omega_{m2} = 0.95\,\omega_m$ (red sphere line), and $\omega_{m2} = 1.05\,\omega_m$ (blue diamond line), respectively. In order to make a comparison, we also plot E_N when $\omega_{m1} = \omega_{m2} = \omega_m$ (purple hexagram line). The figures show that whether the OPA exists or not, the influence of 5% frequency deviation of ω_{m2} on the entanglement between the two oscillators separated in space is similar. When the frequency of $B_2 \omega_{m2} = 0.95\,\omega_m$ (red sphere line), the entanglement between the oscillators is slightly enhanced. While when $\omega_{m2} = 1.05\,\omega_m$ (blue diamond line), the entanglement is slightly decreased and optimal entanglement is slightly shifted towards higher detuning value. More importantly, the robustness of entanglement against environment temperature is stronger along with the enhanced entanglement when $\omega_{m2} = 0.95\,\omega_m$. The above discussion indicates that the slight frequency deviation between the oscillators not only cannot affect the classical-to-quantum transition behavior between two oscillators separated in space from experimental point, but also implies that we can control the strength of entanglement and the optimal entanglement occurrence through adjusting the frequencies of the two oscillators.

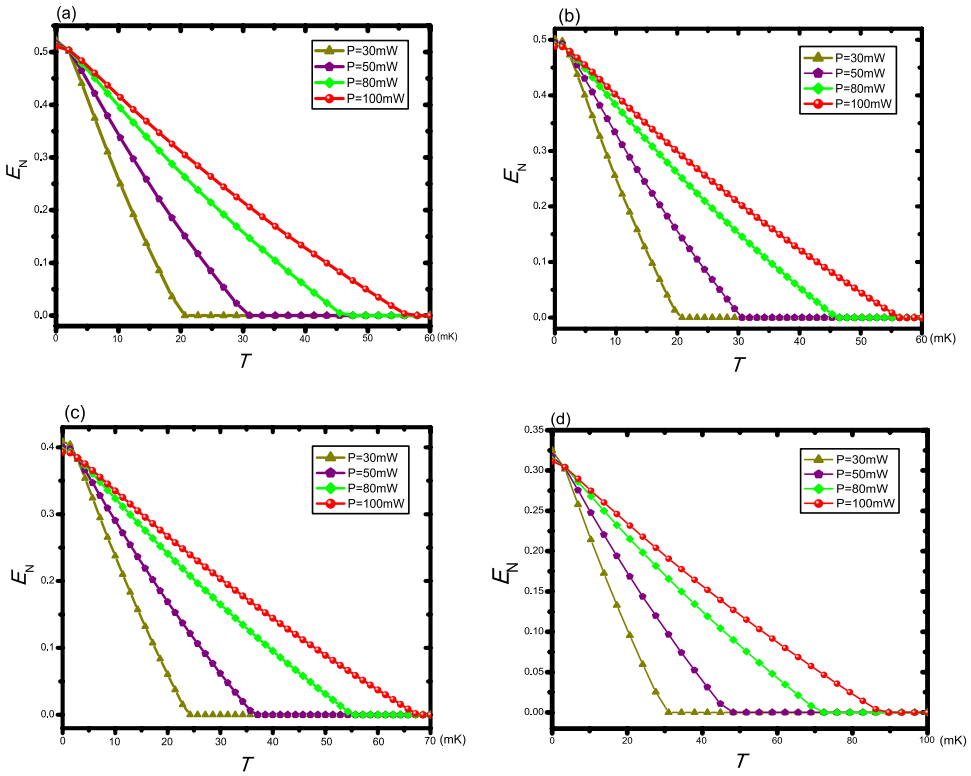

Figure 5. Plot of the logarithmic negativity E_N as a function of the temperature for four different values of the laser power $P = 30$ mW (dark yellow triangle line), $P = 50$ mW (purple pentagon line), $P = 80$ mW (green diamond line), and $P = 100$ mW (red sphere line). Here we set $\lambda = 0.95\,\omega_m$, $\Delta = 0.75\,\omega_m$, $\theta = \pi/16$, and $C_g = 0$, 2×10^7 Hz, 8×10^7 Hz, 12×10^7 Hz, respectively, in (**a**–**d**).

Last but not least, we note that Eq. (4) does't contain the quadratic terms $q_j^2 (j = 1, 2)$ which arise from the Eq. (2), i.e., the effect of the frequency shift caused by the Coulomb interaction between the two charged oscillators. In practice, the influence of the quadratic terms $q_j^2 (j = 1, 2)$ in Eq. (2) is to readjust the frequency of the oscillators. Hence, it is significant necessary to discuss the effect of the frequency shift caused by the Coulomb interaction. During the above analysis, we have chosen the maximum coefficient of $\hbar q_1 q_2$ term as $0.95\,\omega_m$. To realize the present scheme, therefore, we should choose the frequency of the oscillator once again to supplement the negative frequency shift due to the Coulomb interaction. The new frequency of the oscillator approximately approaches to $280\,\pi$MHz because it is just the required oscillator in our scheme when taken the frequency shift due to the Coulomb interaction into account. It is worthy to point out that, with the fast development of the micro-nano manufacturing technology, the high-quality and high frequency micro-nano oscillator has been arisen in experiment. Specially, the oscillator of the order of magnitude of the gigahertz has been reported in experiment[66].

In addition, the technology of generation of squeezed photons via the second-order nonlinearity in the cavity has been quite mature now. In 1986, Wu *et al*. has realized the squeezing of photons via the degenerate parametric amplifier in the cavity experimentally[67]. Methods for detection of entanglement have been discussed[17,20], and the entanglement properties between the oscillators can be verified by experimentally measuring the corresponding covariance matrix. It can be achieved by combining existing experimental techniques. The mechanical position and momentum can be measured with the setup proposed in ref. 49 in which via adjusting the detuning and bandwidth of an additional adjacent cavity, both position and momentum of the oscillator can be measured by homodyning the output of the second cavity.

Conclusion

In conclusion, we have proposed a scheme to show that the system consisting of two macroscopic oscillators separated in space which are coupled through Coulomb interaction displays the classical-to-quantum transition behavior under the action of optomechanical coupling interaction. Our investigation indicates that once the optomechanical coupling interaction disappears, the entanglement between the two separated oscillators disappears accordingly and the system will return to classical world even though there exists sufficiently strong Coulomb coupling between the oscillators. Resorting to the squeezing of the cavity field generated by an OPA inside the cavity, we also consider the case of squeezed light driving and discuss the effect of squeezed light driving on this classical-to-quantum transition behavior instead of injecting the squeezed field directly. We find that even though the squeezed light driving cannot enhance the strength of the classical-to-quantum transition behavior, it considerably increases the robustness against the environment temperature of this transition behavior. We also find that in the case of ordinary light driving or squeezed light driving, the slight frequency deviation

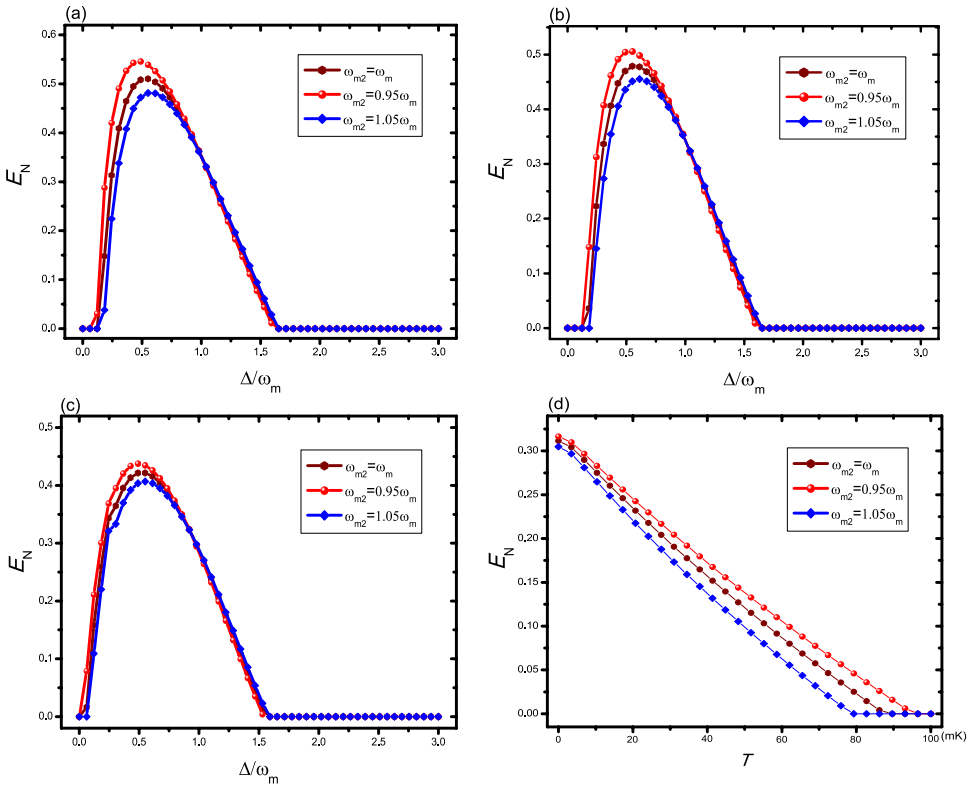

Figure 6. Plot of the logarithmic negativity E_N when the frequencies of two oscillators are different. (**a**) $\lambda = 0.95\,\omega_m$ and other parameters are same with Fig. 2; (**b**) $C_g = 2 \times 10^7$ Hz and other parameters are same with Fig. 3; (**c**) $C_g = 8 \times 10^7$ Hz, $\theta = \pi/4$, and other parameters are same with Fig. 4; (**d**) $P = 100$ mW and other parameters are same with Fig. 5(d).

between the oscillators not only cannot affect the occurrence of this classical-to-quantum transition behavior, but also implies to control the strength of entanglement and optimal entanglement occurrence through adjusting the frequencies of the two separated oscillators. In current experimentally feasible regimes, the results of numerical simulation show that the present scheme is feasible and practical and has stronger robustness compared with previous schemes. It is promising that the scheme might possibly help us to further clarify and grasp the classical-quantum boundary.

References

1. Schrödinger, E. Discussion of Probability Relations between Separated Systems. *Proc. Cambridge Philos. Soc.* **31**, 555, doi:10.1017/S0305004100013554 (1935).
2. Horodecki, R., Horodecki, P., Horodecki, M. & Horodecki, K. Quantum entanglement. *Rev. Mod. Phys.* **81**, 865–942, doi:10.1103/RevModPhys.81.865 (2009).
3. Jones, J. A. & Jaksch, D. *Quantum Information, Computation and Communication* (Cambridge University Press, Cambridge, UK, 2012).
4. Giovannetti, V., Lloyd, S. & Maccone, L. Advances in quantum metrology. *Nat. Photon.* **5**, 222–229, doi:10.1038/nphoton.2011.35 (2011).
5. Wang, H. F., Zhu, A. D., Zhang, S. & Yeon, K. H. Simple implementation of discrete quantum Fourier transform via cavity quantum electrodynamics. *New J. Phys.* **13**, 013021, doi:10.1088/1367-2630/13/1/013021 (2011).
6. Sun, W. M. *et al.* Dissipative preparation of three-atom entanglement state via quantum feedback control. *J. Opt. Soc. Am. B* **32**, 9 (2015).
7. Su, S. L., Shao, X. Q., Wang, H. F. & Zhang, S. Scheme for entanglement generation in an atom-cavity system via dissipation. *Phys. Rev. A* **90**, 054302, doi:10.1103/PhysRevA.90.054302 (2014).
8. Su, S. L., Shao, X. Q., Wang, H. F. & Zhang, S. Preparation of three-dimensional entanglement for distant atoms in coupled cavities via atomic spontaneous emission and cavity decay. *Sci. Rep.* **4**, 7566, doi:10.1038/srep07566 (2014).
9. Su, S. L., Guo, Q., Wang, H. F. & Zhang, S. Simplified scheme for entanglement preparation with Rydberg pumping via dissipation. *Phys. Rev. A* **92**, 022328, doi:10.1103/PhysRevA.92.022328 (2015).
10. Wang, H. F. & Zhang, S. Linear optical generation of multipartite entanglement with conventional photon detectors. *Phys. Rev. A* **79**, 042336, doi:10.1103/PhysRevA.79.042336 (2009).
11. Wang, H. F. & Zhang, S. Scheme for linear optical preparation of a type of four-photon entangled state with conventional photon detectors. *Eur. Phys. J. D* **53**, 359–363, doi:10.1140/epjd/e2009-00129-2 (2009).
12. Wang, H. F., Zhang, S., Zhu, A. D., Yi, X. X. & Yeon, K. H. Local conversion of four Einstein-Podolsky-Rosen photon pairs into four-photon polarization-entangled decoherence-free states with non-photon-number-resolving detectors. *Opt. Express* **19**, 25433–40, doi:10.1364/OE.19.025433 (2011).
13. Cirac, J. I. & Zoller, P. Quantum computations with cold trapped ions. *Phys. Rev. Lett.* **74**, 4091–4094, doi:10.1103/PhysRevLett.74.4091 (1995).

14. Kielpinski, D., Monroe, C. & Wineland, D. J. Architecture for a large-scale ion-trap quantum computer. *Nature (London)* **417**, 709–711, doi:10.1038/nature00784 (2002).
15. Wilson, A. C. *et al*. Tunable spin-spin interactions and entanglement of ions in separate potential wells. *Nature (London)* **512**, 57–60, doi:10.1038/nature13565 (2014).
16. Chen, L. B., Shi, P., Zheng, C. H. & Gu, Y. J. Generation of three-dimensional entangled state between a single atom and a Bose-Einstein condensate via adiabatic passage. *Opt. Express* **20**, 14547–55, doi:10.1364/OE.20.014547 (2012).
17. Mancini, S., Giovannetti, V., Vitali, D. & Tombesi, P. Entangling macroscopic oscillators exploiting radiation pressure. *Phys. Rev. Lett.* **88**, 120401, doi:10.1103/PhysRevLett.88.120401 (2002).
18. Huang, S. & Agarwal, G. S. Entangling nanomechanical oscillators in a ring cavity by feeding squeezed light. *New J. Phys.* **11**, 103044, doi:10.1088/1367-2630/11/10/103044 (2009).
19. Zhang, J., Peng, K. & Braunstein, S. L. Quantum-state transfer from light to macroscopic oscillators. *Phys. Rev. A* **68**, 013808, doi:10.1103/PhysRevA.68.013808 (2003).
20. Pinard, M. *et al*. Entangling movable mirrors in a double-cavity system. *Europhys. Lett.* **72**, 747–753, doi:10.1209/epl/i2005-10317-6 (2005).
21. Vitali, D., Mancini, S. & Tombesi, P. Stationary entanglement between two movable mirrors in a classically driven Fabry-Perot cavity. *J. Phys. A: Math. Theor* **40**, 8055–8068, doi:10.1088/1751-8113/40/28/S14 (2007).
22. Hartmann, M. J. & Plenio, M. B. Steady state entanglement in the mechanical vibrations of two dielectric membranes. *Phys. Rev. Lett.* **101**, 200503, doi:10.1103/PhysRevLett.101.200503 (2008).
23. Liao, J. Q., Wu, Q. Q. & Nori, F. Entangling two macroscopic mechanical mirrors in a two-cavity optomechanical system. *Phys. Rev. A* **89**, 014302, doi:10.1103/PhysRevA.89.014302 (2014).
24. Tan, H., Buchmann, L. F., Seok, H. & Li, G. Achieving steady-state entanglement of remote micromechanical oscillators by cascaded cavity coupling. *Phys. Rev. A* **87**, 022318, doi:10.1103/PhysRevA.87.022318 (2013).
25. Buchmann, L. F. & Stamper-Kurn, D. M. Nondegenerate multimode optomechanics. *Phys. Rev. A* **92**, 013851, doi:10.1103/PhysRevA.92.013851 (2015).
26. Li, J., Haghighi, I. M., Malossi, N., Zippilli, S. & Vitali, D. Generation and detection of large and robust entanglement between two different mechanical resonators in cavity optomechanics. *New J. Phys.* **17**, 103037, doi:10.1088/1367-2630/17/10/103037 (2015).
27. Li, J., Hou, B., Zhao, Y. & Wei, L. Enhanced entanglement between two movable mirrors in an optomechanical system with nonlinear media. *Europhys. Lett.* **110**, 64004, doi:10.1209/0295-5075/110/64004 (2015).
28. Bai, C. H., Wang, D. Y., Wang, H. F., Zhu, A. D. & Zhang, S. Robust entanglement between a movable mirror and atomic ensemble and entanglement transfer in coupled optomechanical system. *Sci. Rep* **6**, 33404, doi:10.1038/srep33404 (2016).
29. Schwab, K. C. & Roukes, M. L. Putting mechanics into quantum mechanics. *Phys. Today* **58**, 36–42, doi:10.1063/1.2012461 (2005).
30. Zurek, W. H. Decoherence and the Transition from Quantum to Classical. *Phys. Today* **44**, 36–44, doi:10.1063/1.881293 (1991).
31. O'Connell, A. D. *et al*. Quantum ground state and single-phonon control of a mechanical resonator. *Nature (London)* **464**, 697–703, doi:10.1038/nature08967 (2010).
32. Teufel, J. D. *et al*. Sideband cooling of micromechanical motion to the quantum ground state. *Nature (London)* **475**, 359–63, doi:10.1038/nature10261 (2011).
33. Chan, J. *et al*. Laser cooling of a nanomechanical oscillator into its quantum ground state. *Nature (London)* **478**, 89–92, doi:10.1038/nature10461 (2011).
34. Wang, D. Y., Bai, C. H., Wang, H. F., Zhu, A. D. & Zhang, S. Steady-state mechanical squeezing in a hybrid atom-optomechanical system with a highly dissipative cavity. *Sci. Rep.* **6**, 24421, doi:10.1038/srep24421 (2016).
35. Wang, D. Y., Bai, C. H., Wang, H. F., Zhu, A. D. & Zhang, S. Steady-state mechanical squeezing in a double-cavity optomechanical system. *Sci. Rep.* **6**, 38559, doi:10.1038/srep38559 (2016).
36. Huang, S. & Agarwal, G. S. Enhancement of cavity cooling of a micromechanical mirror using parametric interactions. *Phys. Rev. A* **79**, 013821, doi:10.1103/PhysRevA.79.013821 (2009).
37. Huang, S. & Agarwal, G. S. Normal-mode splitting in a coupled system of a nanomechanical oscillator and a parametric amplifier cavity. *Phys. Rev. A* **80**, 033807, doi:10.1103/PhysRevA.80.033807 (2009).
38. Agarwal, G. S. & Huang, S. Strong mechanical squeezing and its detection. *Phys. Rev. A* **93**, 043844, doi:10.1103/PhysRevA.93.043844 (2016).
39. Peano, V., Schwefel, H. G. L., Marquardt, C. & Marquardt, F. Intracavity Squeezing Can Enhance Quantum-Limited Optomechanical Position Detection through Deamplification. *Phys. Rev. Lett.* **115**, 243603, doi:10.1103/PhysRevLett.115.243603 (2015).
40. Scully, M. O. & Zubairy, M. S. *Quantum Optics* (Cambridge University Press 1997).
41. Walls, D. F. & Milburn, G. J. *Quantum Optics* (Springer-Verlag Berlin Heidelberg 1994).
42. Xue, Z. Y., Yang, L. N. & Zhou, J. Circuit electromechanics with single photon strong coupling. *Applied Physics Letters* **107**, 023102, doi:10.1063/1.4926506 (2015).
43. Zhou, J. *et al*. High fidelity quantum state transfer in electromechanical systems with intermediate coupling. *Sci. Rep* **4**, 6237, doi:10.1038/srep06237 (2014).
44. Hensinger, W. K. *et al*. Ion trap transducers for quantum electromechanical oscillators. *Phys. Rev. A* **72**, 041405(R), doi:10.1103/PhysRevA.72.041405 (2005).
45. Zhang, J. Q., Li, Y., Feng, M. & Xu, Y. Precision measurement of electrical charge with optomechanically induced transparency. *Phys. Rev. A* **86**, 053806, doi:10.1103/PhysRevA.86.053806 (2012).
46. Ma, P. C., Zhang, J. Q., Xiao, Y., Feng, M. & Zhang, Z. M. Tunable double optomechanically induced transparency in an optomechanical system. *Phys. Rev. A* **90**, 043825, doi:10.1103/PhysRevA.90.043825 (2014).
47. Chen, R. X., Shen, L. T. & Zheng, S. B. Dissipation-induced optomechanical entanglement with the assistance of Coulomb interaction. *Phys. Rev. A* **91**, 022326–9, doi:10.1103/PhysRevA.91.022326 (2015).
48. Tian, L. & Zoller, P. Coupled ion-nanomechanical systems. *Phys. Rev. Lett.* **93**, 266403, doi:10.1103/PhysRevLett.93.266403 (2004).
49. Vitali, D. *et al*. Optomechanical entanglement between a movable mirror and a cavity field. *Phys. Rev. Lett.* **98**, 030405, doi:10.1103/PhysRevLett.98.030405 (2007).
50. Genes, C., Vitali, D. & Tombesi, P. Emergence of atom-light-mirror entanglement inside an optical cavity. *Phys. Rev. A* **77**, 050307(R), doi:10.1103/PhysRevA.77.050307 (2008).
51. Giovannetti, V. & Vitali, D. Phase-noise measurement in a cavity with a movable mirror undergoing quantum Brownian motion. *Phys. Rev. A* **63**, 023812, doi:10.1103/PhysRevA.63.023812 (2001).
52. Aspelmeyer, M., Kippenberg, T. J. & Marquardt, F. Cavity optomechanics. *Rev. Mod. Phys.* **86**, 1391–1452, doi:10.1103/RevModPhys.86.1391 (2014).
53. Fabre, C. *et al*. Quantum-noise reduction using a cavity with a movable mirror. *Phys. Rev. A* **49**, 1337–1343, doi:10.1103/PhysRevA.49.1337 (1994).
54. Hurwitz, A. In *Selected Papers on Mathematical Trends in Control Theory* edited by Bellman, R. & Kalaba, R. (Dover, New York, 1964).
55. DeJesus, E. X. & Kaufman, C. Routh-Hurwitz criterion in the examination of eigenvalues of a system of nonlinear ordinary differential equations. *Phys. Rev. A* **35**, 5288–5290, doi:10.1103/PhysRevA.35.5288 (1987).
56. Weedbrook, C. *et al*. Gaussian quantum information. *Rev. Mod. Phys.* **84**, 621–669, doi:10.1103/RevModPhys.84.621 (2012).

57. Adesso, G. & Illuminati, F. Entanglement in continuous-variable systems: recent advances and current perspectives. *J. Phys. A* **40**, 7821 (2007).
58. Vidal, G. & Werner, R. F. Computable measure of entanglement. *Phys. Rev. A* **65**, 032314, doi:10.1103/PhysRevA.65.032314 (2002).
59. Adesso, G., Serafini, A. & Illuminati, F. Extremal entanglement and mixedness in continuous variable systems. *Phys. Rev. A* **70**, 022318, doi:10.1103/PhysRevA.70.022318 (2004).
60. Plenio, M. B. Logarithmic negativity: a full entanglement monotone that is not convex. *Phys. Rev. Lett.* **95**, 090503, doi:10.1103/PhysRevLett.95.090503 (2005).
61. Simon, R. Peres-Horodecki separability criterion for continuous variable systems. *Phys. Rev. Lett.* **84**, 2726–9, doi:10.1103/PhysRevLett.84.2726 (2000).
62. Schliesser, A., Riviere, R., Anetsberger, G., Arcizet, O. & Kippenberg, T. J. Resolved-sideband cooling of a micromechanical oscillator. *Nat. Phys.* **4**, 415–419, doi:10.1038/nphys939 (2008).
63. Gigan, S. *et al*. Self-cooling of a micromirror by radiation pressure. *Nature (London)* **444**, 67–70, doi:10.1038/nature05273 (2006).
64. Agarwal, G. S. & Adam, G. Photon distributions for nonclassical fields with coherent components. *Phys. Rev. A* **39**, 6259–6266, doi:10.1103/PhysRevA.39.6259 (1989).
65. Teufel, J. D. *et al*. Circuit cavity electromechanics in the strong-coupling regime. *Nature (London)* **471**, 204–8, doi:10.1038/nature09898 (2011).
66. Chan, J. *et al*. Laser cooling of a nanomechanical oscillator into its quantum ground state. *Nature (Lodon)* **478**, 89–92, doi:10.1038/nature10461 (2011).
67. Wu, L. A., Kimble, H. J., Hall, J. L. & Wu, H. Generation of Squeezed States by Parametric Down Conversion. *Phys. Rev. Lett.* **57**(20), 2520–2523, doi:10.1103/PhysRevLett.57.2520 (1986).

Acknowledgements

This work was supported by the National Natural Science Foundation of China under Grant Nos 11264042, 11465020, 61465013, 11564041, and the Project of Jilin Science and Technology Development for Leading Talent of Science and Technology Innovation in Middle and Young and Team Project under Grant No. 20160519022JH.

Author Contributions

C.-H.B. designed the scheme under the guidance of H.-F.W., A.-D.Z., and S.Z., C.-H.B. and D.-Y.W. carried out the theoretical analysis. All authors contributed to the interpretation of the work and the writing of the manuscript. All authors reviewed the manuscript.

Additional Information

Competing Interests: The authors declare that they have no competing interests.

Publisher's note: Springer Nature remains neutral with regard to jurisdictional claims in published maps and institutional affiliations.